Short Communication

Development of Ag/ZnO nanorods and nanoplates at low hydrothermal temperature and time for acetone sensing application: an insight into spillover mechanism

Digambar Y. Nadargi[1] · Mohaseen S. Tamboli[2] · Santosh S. Patil[3] · Imtiaz S. Mulla[4] · Sharad S. Suryavanshi[1]

Received: 23 July 2019 / Accepted: 24 October 2019 / Published online: 6 November 2019

Abstract
Nanostructure synthesis at low temperature with high purity and yield has a great potential in the present competitive research and development of nanomaterials for varieties of application. Here, we demonstrate the facile hydrothermal synthesis of ZnO nanocomposites at low hydrothermal temperature and time. With barely 80 °C hydrothermal temperature and 2 h of reaction time, ZnO nanorods were successfully synthesized, while by slightly increasing the reaction time (6 h-and-on), nanoplates of the same material were developed. Both the obtained nanostructures were analyzed using physio-chemical characterizing tools and examined for practical relevance as gas sensing material. The optimized sample was further treated to Ag loading (1–5 mol%) for lowering the operating temperature of the sensor. ZnO sample with 3 mol% Ag loading showed excellent sensitivity of 92.7% for 1000 ppm of acetone concentration with a drop in the operating temperature from 325 °C (Pristine ZnO) to 250 °C (Ag-loaded ZnO). The morphological correlation with reaction time and thereby sensitivity and spillover mechanism are discussed.

Electronic supplementary material The online version of this article (https://doi.org/10.1007/s42452-019-1573-2) contains supplementary material, which is available to authorized users.

✉ Sharad S. Suryavanshi, sssuryavanshi@rediffmail.com | [1]School of Physical Sciences, Punyashlok Ahilyadevi Holkar Solapur University, Solapur 413255, India. [2]Department of Chemistry and Research Institute for Natural Sciences, Hanyang University, 222 Wangsimni-ro, Seongdong-gu, Seoul 04763, Republic of Korea. [3]Department of Chemistry, Pohang University of Science and Technology (POSTECH), Pohang 37673, Republic of Korea. [4]Former Emeritus Scientist (CSIR), Centre for Materials for Electronics Technology, Pune 411008, India.

Graphic abstract

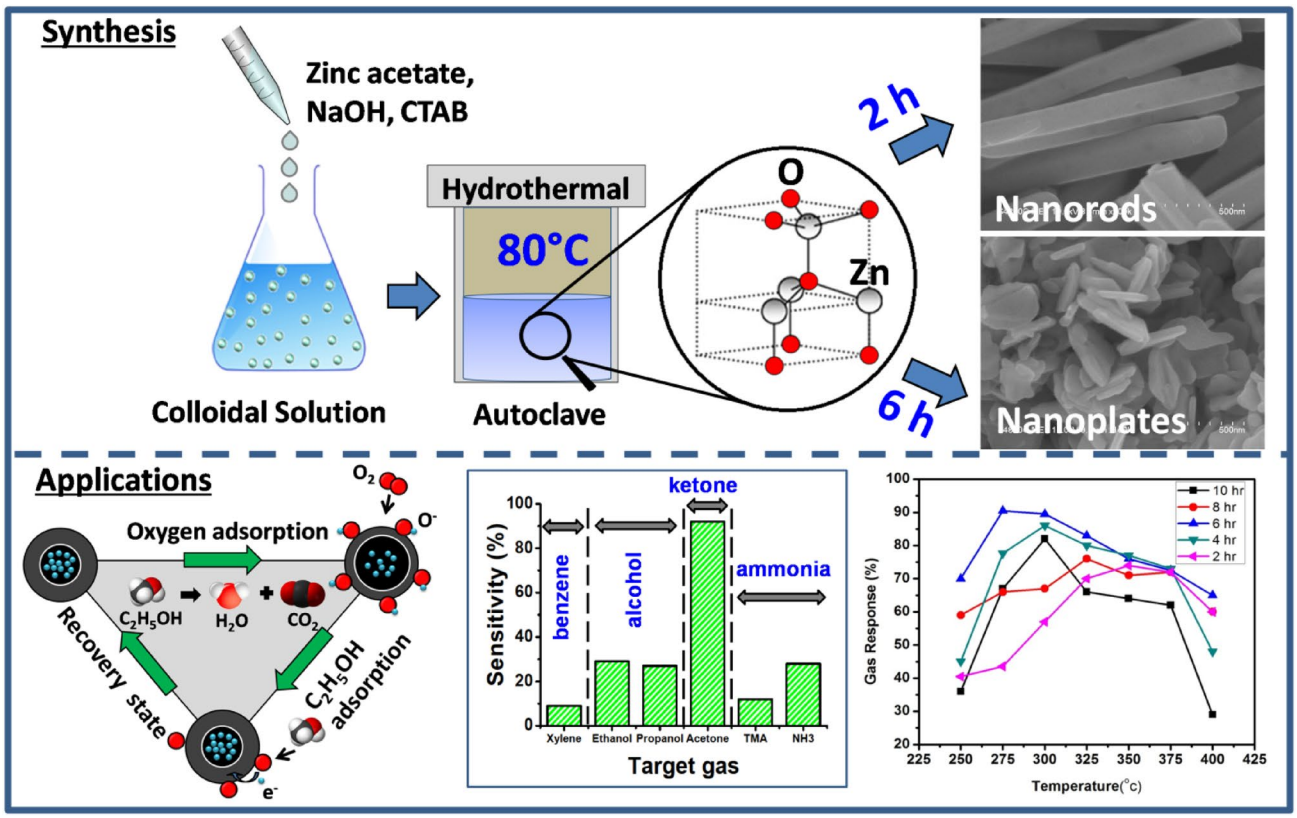

Keywords Composite materials · Hydrothermal process · Ag/ZnO · Sensors · Acetone

1 Introduction

Since the discovery of ZnO and its usefulness in varieties of applications, it has attracted increasing attention as promising semiconducting material [1–5]. Apart from gas sensing, ZnO has attracted high technological applications, like photodetectors, photodiodes, surface acoustic wave filters, solar cells, photonic crystals, LEDs, optical waveguides, due to its wide direct band gap (3.3 eV) and large excitation binding energy (60 meV) [6–12]. In the state of the art, doping of noble metals like gold (Au), platinum (Pt), ruthenium (Ru), nickel (Ni), palladium (Pd), gallium (Ga), silver (Ag) and their combinations showed significant improvement in ZnO-based gas sensor [13–20]. The loading of these noble metals into parent metal oxide amplifies the charge transfer mechanism. Amongst the noble metals, silver is one of the best candidates for loading into ZnO matrix, due to its least orbital energy, better solubility and larger ionic size. In comparison with other noble metals, Ag boosts the catalytic activities and thereby surface reactions.

However, in the present industrial scenario, chemical synthesis of these nanomaterials is facing enormous challenges in terms of trimming the overall process span and production at low temperature. Though hydrothermal synthesis route offers decent advantages over conventional synthesis routes, its high reaction temperature (hence high pressure) and longer reaction time are the major concerns at pilot/industrial-scale production. However, by effective tuning of reaction temperature in combination with the reaction time, one can get the same nanomaterial in the desired morphology. Here, the problem addressed in the paper is to ease the high temperature and time-consuming process for synthesizing ZnO-based nanostructures. The efforts were made to custom tailor the ZnO nanostructures at lower hydrothermal temperature (80 °C) and shorter reaction time (2–10 h). With barely 80 °C hydrothermal temperature and 2 h of reaction time, ZnO nanorods were successfully synthesized, while by slightly increasing the reaction time (6 h-and-on), nanoplates of the same material were developed. The obtained nanostructures are

Table 1 Summary of hydrothermally developed ZnO nanostructures at various reaction temperature and time

#	Hydrothermal reaction		Obtained nanostructures	References
	Temperature (°C)	Time (h)		
1	150	8	Nanorods	[21]
2	120	20	Nanorods	[22]
3	160	20	Nanoplates	[22]
4	100	5	Nanoparticles	[23]
5	90	20	Nanorods	[24]
6	90	5	Nanorods	[25]
7	80	2	Nanorods	Our efforts
8	80	6	Nanoplates	Our efforts

further loaded with Ag for their potential application in gas sensing analysis at lower operating temperature (due to spillover mechanism). Table 1 summarizes the results of hydrothermally developed ZnO nanostructures, where our efforts are highly remarkable.

2 Experimental procedure and characterizations

For the development of sensor material, zinc acetate dihydrate $Zn(CH_3COO)_2{\cdot}2H_2O$, silver nitrate ($AgNO_3$), sodium hydroxide (NaOH) and cetyltrimethylammonium bromide (CTAB) ($CH_3(CH_2)_{15}N(Br)(CH_3)_3$) were purchased from Sigma-Aldrich and used as is. The facile synthesis route took up for the sensor development was hydrothermal strategy (Fig. 1). Pristine ZnO samples were prepared by dissolving $Zn(CH_3COO)_2{\cdot}2H_2O$ (2.10 g, 10 mmol) in 48 ml of NaOH(1 M) upon constant stirring. A separately prepared surfactant solution (CTAB, 2.5 gm in 42 ml distilled water (DW) and 30 ml ethanol) was added to reacting solvent, with constant stirring. After 30 min, white turbid solution was obtained, which then transferred to autoclave assemble made up of Teflon liner. The hydrothermal reaction was carried out at 80 °C with varying reaction timings, viz. 2–10 h (Step-2h). For Ag loading (1, 3 and 5 mol%), a respective amount of $AgNO_3$ was added to reacting mixture, prior to surfactant addition. The precipitate (white: for pristine ZnO, grey: for Ag/ZnO) was obtained, after cooling down the autoclave at room temperature. The precipitate was washed with DW and ethanol, followed by drying at 60 °C in air for 2 h in normal oven. Dried powders were grounded and subsequently annealed in air at 400 °C for 2 h in air. Finally, samples were labelled as H2, H4, H6, H8 and H10 for hydrothermal reaction time of 2–10 h, respectively. Similarly, Ag/ZnO sample (sample H6) with 1, 3 and 5 mol% Ag loading was labelled as A1, A3 and A5, respectively. For gas sensing analysis, the thick films of developed material were fabricated on the alumina substrates, using screen printing technique (Fig. S1). Finally, the films were sintered at 400 °C at 1 h in air to remove the added binders from the thixotropic paste.

3 Results and discussion

The XRD analyses of the developed sensor materials are highlighted in Fig. 2a, b. Part-A shows the XRD image of pristine ZnO (sample H6) along with the JCPDS (#36-1451) lines. In contrast, Part-B shows the XRD images of Ag/ZnO samples (A1,A3,A5) with different mol% of Ag. The obtained XRD signatures indicate the wurtzite structure with the crystal planes (100), (002), (101), (102), (110), (103), (112) which are corresponding to JCPDS file No. 36-1451. The additional peak (200) is corresponding to Ag element in the ZnO matrix. The emergence of Ag_2O peak corresponding to (111) at $2\theta \sim 32$ is in accordance with JCPDS No. 41-1104. The XRD shows formation of highly oriented peak along (002) plane indicating highly crystalline material. The crystallites size was obtained 56.10 nm which was determined using full width at half maximum

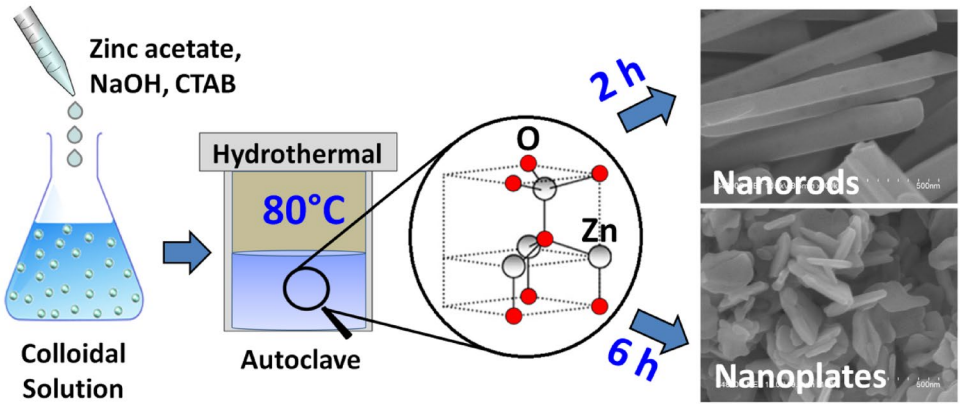

Fig. 1 Schematic illustration for facile development of ZnO nanorods and nanoplates at low hydrothermal temperature (left part) and SEM images of developed nanostructures

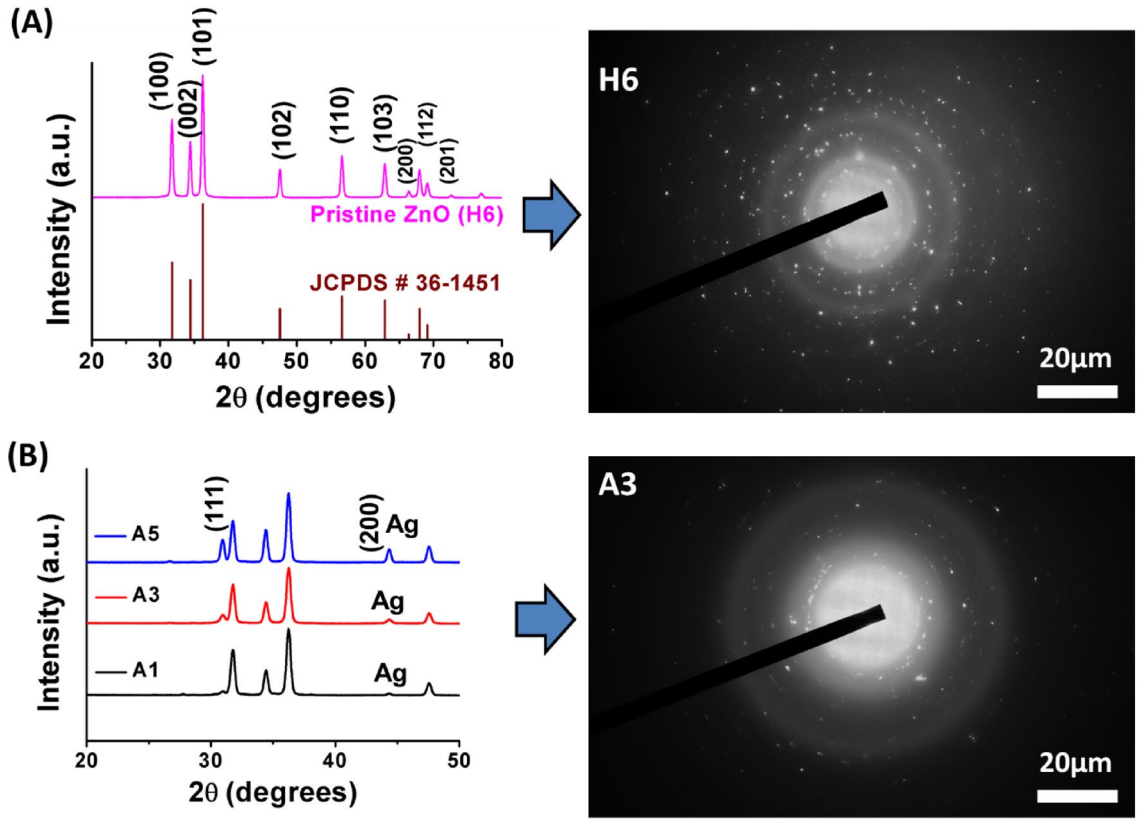

Fig. 2 XRD of ZnO with 6 h hydrothermal reaction along with std. peak reflections (left part); the inset shows the reflection intensities of Ag loadings. SAED pattern of ZnO with 6 h hydrothermal reaction (right part)

(FWHM) for the most intense (101) peak, using Scherrer formula [26].

$$D = 0.9\lambda/\beta\cos\theta \quad (1)$$

where 'β' is FWHM (in radians), 'θ' the angle of reflection and 'λ' the wavelength of X-ray radiation used. Moreover, the bright patterns of SAED (right part: H6 & A3) are matching with wurtzite ZnO planes, thereby revalidating the XRD analyses [27].

The developed material exhibits 1D and 2D nanostructures (nanorods and nanoplates) depending upon the time of hydrothermal reaction (Fig. 3). The bunch of nanorods (Fig. 3H2, H4) were obtained at lower hydrothermal reaction temperature (80 °C) with barely 2–4 h reaction time. These nanorods started to convert into nanoplates after 4 h reaction time (Fig. 3H6, H8, A3). After longer heating duration, the 700–800-nm long and < 100-nm diameter nanorods get converted into 160–200-nm wide and 100–150-nm long nanoplates, with 28–30-nm thickness. Under TEM analysis, the obtained structures seem to have high aspect ratio and size consistent (Fig. 4H4, H6). In particular, the nanoplates were loosely and poriferously aggregated, showing the complimentary tendency to have a better gas sensing performance. The available copious channels provide the effective gas diffusion. EDS analysis of the developed material (Fig. 4H6, A3) confirmed the formation of Ag/ZnO nanocomposites along with the presence of Zn, O and Ag as per their concentrations in the respective samples (Table S1).

As a practical relevance, the developed nanostructures were tested for gas sensing proficiency towards various reducing gases (ethanol, propanol, xylene, trimethylamine, ammonia and acetone). All the materials developed at different hydrothermal reaction time showed increasing gas response up to certain operating temperature, followed by decreasing trend with further increase in the temperature (Fig. 5a). It is due adsorption–desorption reactions of oxygen from the ZnO surface, whose possible gas sensing mechanism is illustrated in the graphical abstract [28]. In general, the process of gas sensing undergoes through following steps [29]:

i. Diffusion of gases to the active region
ii. Adsorption of gases on to active region
iii. Surface reactions
iv. Desorption of reaction products from active region
v. Diffusion of reaction products away from active region.

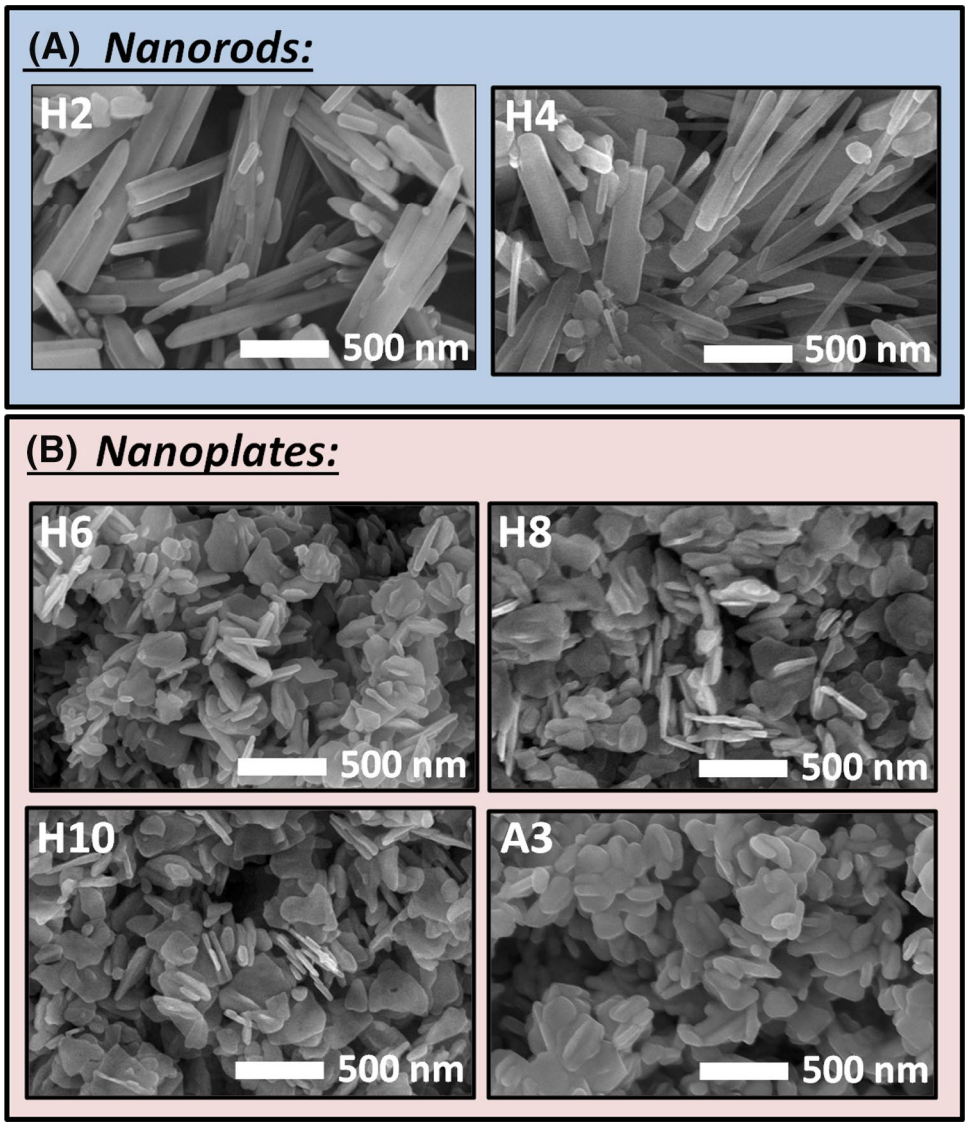

Fig. 3 SEM images of samples H2, H4 as nanorods and samples H6, H8, H10 as nanoplates

The following are the possible reactions for acetone, ammonia and ethanol, respectively.

For acetone:

$$CH_3COCH_3 + 8O^-_{(ads)} \rightarrow 3CO_2 + 3H_2O + 8e^- \quad (2)$$

For ammonia:

$$2NH_3 + 3O^-_{(ads)} \rightarrow 3H_2O + 3e^- + N_2 \uparrow \quad (3)$$

For ethanol:

$$C_2H_5OH + 6O^-_{(ads)} \rightarrow 2CO_2 + 3H_2O + 6e^- \quad (4)$$

In case of having the larger surface area of the sensor, a more number of active sites will be available for adsorption of the target gas. This will, in contrast, release a more number of electrons into the conduction band of ZnO and thereby decrease in the sensor [30]. Remarkable performance distinction was observed amongst developed ZnOs at different hydrothermal treatments (Fig. 5a). Sample H6 showed the highest response (90.5% at 325 °C for 1000 ppm), due to the formation of precise phase (validated in XRD) as well as high surface area in comparison with nanorods (Fig. 4). The BET surface area for sample H4 and sample H6 is obtained as 10.78 m^2/g and 28.31 m^2/g, respectively.

In contrast, higher reaction time (> 6 h) resulted into blocked channels, which trapped the target gas. Therefore, due to unavailability of oxygen vacancy, the gas sensitivity got decreased. Hence, being the optimized pristine sample, Ag loading (1–5 mol%) was carried out in sample H6. By the addition of Ag in the pristine ZnO matrix, gas sensing performance got improved, which is highlighted in Fig. 5b. As expected, though marginal improvement in sensitivity (from 90.5% to 92.7%) was observed, a dramatic fall in the operating temperature (from 325 to 250

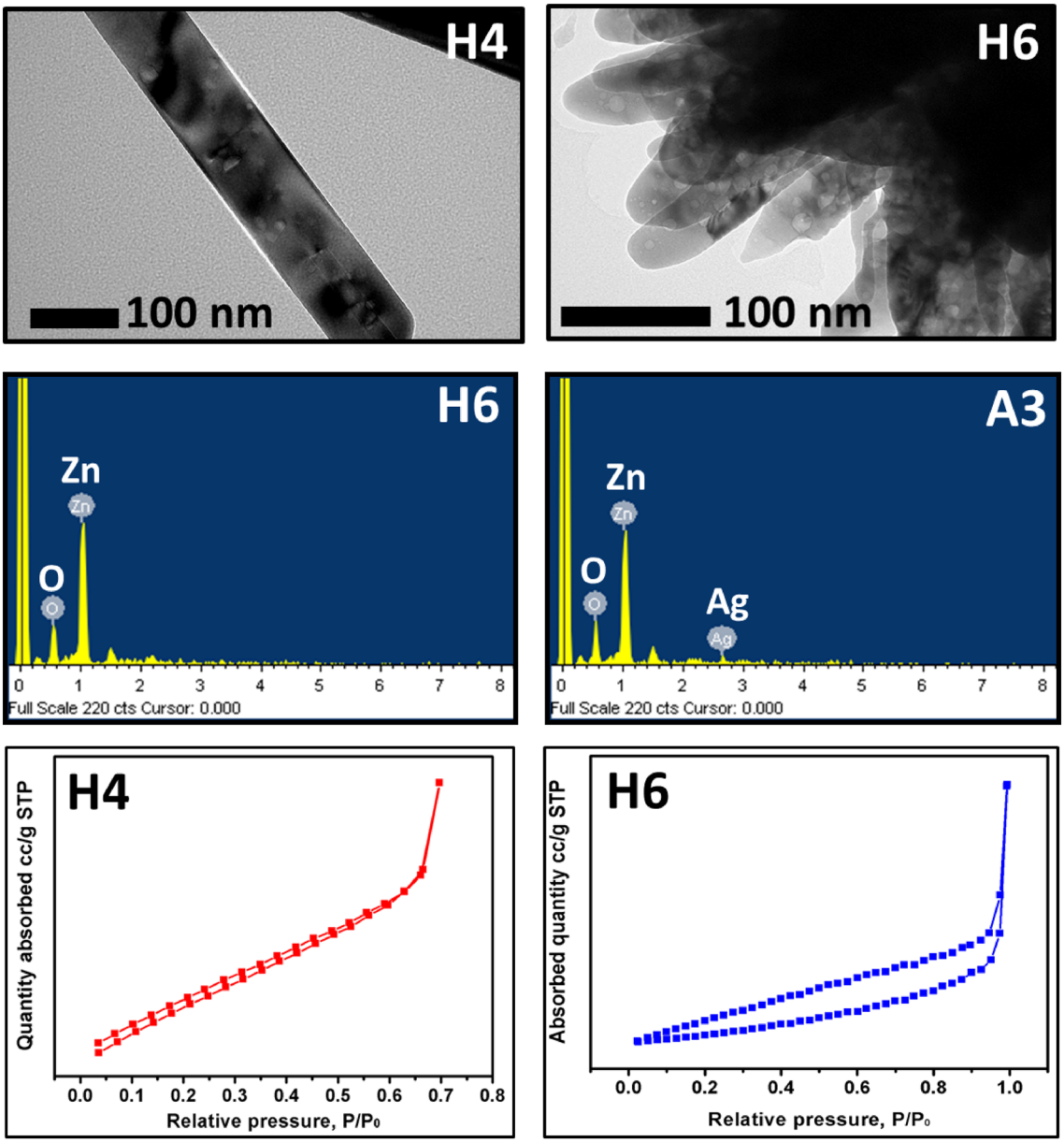

Fig. 4 TEM, SEM and BET analyses of samples H4, H6 and A3

°C) was realized. Thereby, one of the objectives of the present work: to lower down the operating temperature by Ag incorporation was achieved. Amongst the different Ag loadings, sample A3 has the highest response of 92.7% for 1000 ppm. The dots in Fig. 5c describe the maximum value of sensitivity obtained for all the developed samples. The nature of the graph is attributed to the spillover mechanism, due to Ag loading, which is discussed later in the end of this section [31]. With an increase in concentration of Ag (1–3 mol%), more electrons made available (spillover) which helped to have a better control of resistance. However, after threshold level of Ag dosing, the spillover effect got ceased due to agglomeration of nanoparticles [32]. Therefore, Ag loading with 3 mol% in the pristine ZnO was treated as best doping level.

One of the important factors, selectivity, is shown in Fig. 5d. The optimized sample, A3 for gas sensing proficiency towards aforementioned reducing gases, was deduced. From all the target gases, Ag/ZnO demonstrated the best selectivity towards acetone. At an operating temperature of 250 °C, sample showed 92% sensitivity for 1000 ppm acetone concentration over the other target

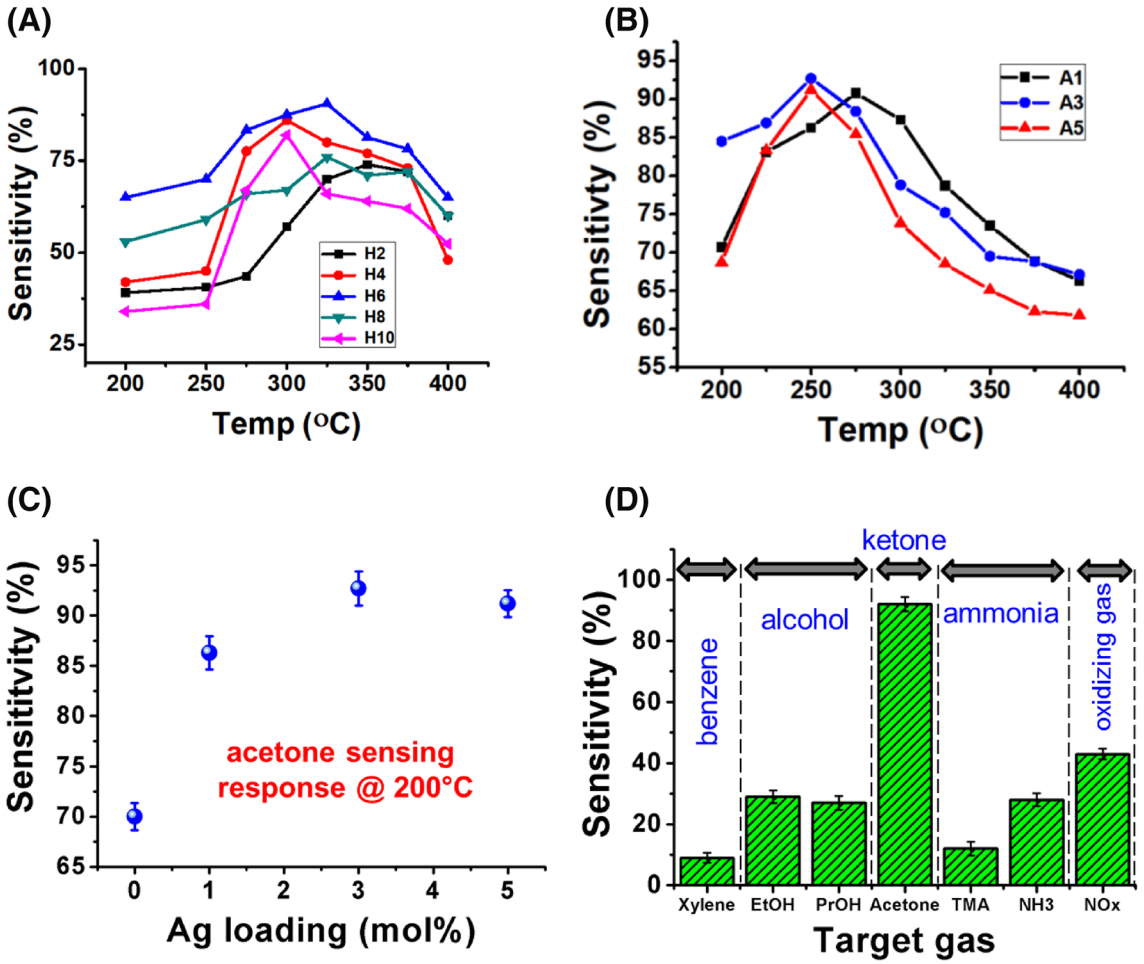

Fig. 5 Gas response properties of the developed materials. **a** acetone sensitivity of pristine ZnOs (H2–H10), **b** acetone sensitivity of Ag-loaded ZnOs (A1–A5) as function of operating temperature, **c** effect of Ag loading on gas response @ 200 °C and **d** selectivity analysis of the optimized sample A3 for various reducing gases

gases. This is due to the lighter nature of acetone which enables faster reaction steps (adsorption, diffusion and desorption) that all are involved in gas sensing mechanism, mentioned above.

The sensor response towards variant concentration (100–2000 ppm acetone) of acetone is highlighted in the supplementary information section (Fig. S4–S6). In general, the sensor response towards acetone increased rapidly up to ~ 500 ppm concentration, and thereafter the increase in response is insignificant. This response behaviour is given by [33]:

$$S = X[Y]^n + K; (n = 0.5 \text{ to } 1.0) \quad (5)$$

where X and K are constants and Y is the concentration of test gas. The value of integer n will be any value between 0.5 and 1.0, according to reaction stoichiometry and surface species charge. This linear relationship is a key prerequisite condition in case of several applications like online gas monitoring.

The related gas sensing evaluation of all the developed sensors and their stability is further highlighted in the supplementary information section (Fig. S7–S10). The gas sensing measurements of H6, A1, A3 and A5 sensors were repeatedly measured on the regular intervals in order to confirm the stability and reproducibility of the sensors. The acetone performance of H6 sensor was measured at an operating temperature of 325 °C towards 1000 ppm concentration of acetone, whereas samples A1–A5 were measured at an operating temperature of 250 °C towards same acetone concentration (1000 ppm). The sensor performance of Ag-loaded ZnO sensors was carried out two times after the initial measurement with the interval of 10 days. It was observed that the sensor responses after 2 months of performance were found to be 90% (H6), 83% (A1), 90% (A3) and 89% (A5), respectively. Thus, the stability and reproducibility were found to be more than 90% in all the samples after 2 months of shelf life. Therefore,

confirm the reproducibility and stability of the developed sensors.

3.1 Spillover mechanism in Ag/ZnO

An improvement in the sensor response can be greatly achieved by the surface modification of metal oxide (ZnO in the present case) either with -(i) doping, -(ii) multicomponent/binary compounds, or (iii) metals/noble metals such as Pd, Au and Ag as a catalyst (Spillover). These methods are highly exploited to enhance the gas sensing performance of metal oxide gas sensors [34–36]. The prime purpose of using these additives is to modify the catalytic activity of the base oxide, favouring the generation of active sites/phases and thereby enhancing the electron exchange rate and as well lowering the operating temperature. By modifying/altering the metal oxide surface through different surface atoms, a new chemical reactivity can be foreseen which enables the sensor to operate at lower temperature. This is the one of the prime motivations of using Ag in the present work that should trigger the spillover process and result into higher response at lower operating temperature.

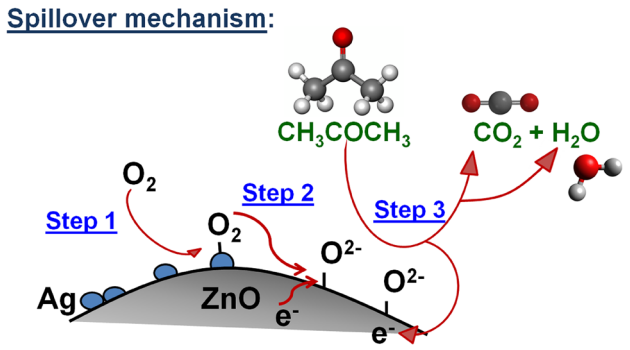

Fig. 6 Schematic illustration of spillover mechanism of Ag/ZnO sensor material for acetone

Herein, emphasis is given to incorporate Ag in ZnO surface, where the support is ZnO whose electrical properties are made to change by active oxidation reactions on its surface. Spillover is a mechanism where the oxidation of reducing agent can be accelerated on the semiconductor surface at much lower temperatures by the presence of dispersed metallic catalyst (Ag in the present case). Ag acts as surface sites for adsorbates and promoters to trigger the surface catalysis. They create additional adsorption sites and surface electronic states. This in turn enhances the gas sensitivity, selectivity and rate of response. 1 mol% doping of Ag led the ZnO to operate at 275 °C from its pristine value of 325 °C. With further increase in the doping (3 mol%), the operating temperature got reduced to 250 °C with an improvement in the response of 92.7% towards acetone. However, the excessive amount of Ag (5 mol%) led to decrease in the response to 91.2% with the same operating temperature of 250 °C. This is due to the change in the functions (catalysis), turning into either shunting layer or active membrane filters, which obstructs the penetration of detecting gas in the surface of ZnO matrix.

The complete gas sensing performance of Ag/ZnO due to spillover mechanism can be explained as follows:

Table 2 Comparative chart for acetone response of ZnO-based material over varying acetone concentration, operating temperature and synthesis route

Sr. No.	Material	Synthesis method	Acetone concentration (ppm)	T_{opt} (°C)	Response	References
1	ZnO	Hydrothermal, 200 °C	100	230	33	[37]
2	Cr–ZnO	RF reactive sputtering	1000 to 15 ppm	300	92% @ 500 ppm	[38]
3	ZnO	Electrospinning	1000	310	1200	[39]
4	Co–ZnO	Electrospinning	100	360	16	[40]
5	ZnO–QDs	Quenching method	500	300	90	[41]
6	ZnO	Hydrothermal, 200 °C	100	300	18.6	[42]
7	ZnO	Refluxing	50	300	16	[43]
8	Co3O4–nO	Hydrothermal, 150 °C	14.7 µM	–	3.58 µAcm – 2 mM – 1	[44]
9	ZnO	Spraying Coating	1000	325	45%	[45]
10	ZnO–Au	Thermal evaporation	200	300	82%	[46]
11	ZnO	Hydrothermal, 180 °C	500	300	10	[47]
12	ZnO–Au	Hydrothermal, 120 °C	100	270	74.41	[48]
13	ZnO	Electrospinning	100	220	67.7	[49]
14	La–ZnO	Precipitation	200	340	60	[50]
15	ZnO	Hydrothermal, 110 °C	100	300	30.4	[51]

Step 1 Oxygen molecules are adsorbed on the Ag surface
Step 2 and spilled over to ZnO, where dissociated oxygen species are ionized with electrons from ZnO.
Step 3 In the presence of target gas, the ionosorbed oxygen reacts with target gas forming a by-product and injecting the electrons back into the conduction band of ZnO. As the concentration of ionosorbed oxygen species is larger on the Ag/ZnO, a larger number of electrons are released to the conduction band under target gas exposure causing a higher sensor signal. The proposed mechanism is illustrated in the following scheme (Fig. 6).

On the context of Occupational Safety and Health Administration (OSHA),(i) Regulatory Limits of acetone are revised on 3/29/2019, with 750 ppm (as STEL Short Term Exposure Limit) and 3000 ppm (Ceiling), and (ii) Recommended Limits are 500 ppm (STEL). Therefore, the following comparative table is made on hydrothermal process as well as other synthesis routes with varying acetone concentration. The obtained results though not tested at 500 ppm are compared with the state-of-art articles, which support the positive outcome of the efforts made so far in developing the nanorods and nanoplates barely at 80 °C. Further, the supporting information of the manuscript gives the detailed graphs on Response as a function of acetone concentration in the range of 100–2000 ppm (Table 2).

4 Conclusion

In conclusion, we demonstrated the facile hydrothermal synthesis of ZnO nanocomposites at lower hydrothermal temperature. The obtained nanorods (at 80 °C, 2–4 h) and nanoplates (at 80 °C, > 4 h) were analyzed through XRD, SEM/TEM, SAED and EDS analyses. As the material holds two distinct morphologies, gas sensing competence was found different for different hydrothermal reaction time. ZnO sample with 3 mol% Ag loading showed excellent sensitivity of 92.7% for 1000 ppm of acetone concentration with a drop in the operating temperature from 325 to 250 °C. Further, the spillover mechanism of Ag/ZnO is explained using schematic illustration by taking acetone as an example of target gas. The reported approach of fabricating gas sensor is easily reproducible at relatively lower cost and thus offers great promise for future industrial application of gas sensors.

Acknowledgements The authors greatly acknowledge to CSIR, India, for the financial support of this work (03(1389)/16/EMR-II). Dr. Nadargi acknowledges CSIR, India, for awarding Research Associate under the same scheme.

Compliance with ethical standards

Conflict of interest The authors declare that there is no competing interest whatsoever.

References

1. Rezk MY, Allam NK (2019) Unveiling the synergistic effect of ZnO nanoparticles and surfactant colloids for enhanced oil recovery. Colloid Interface Sci Commun 29:33
2. Lan S, Sheng X, Lu Y, Li C, Zhao S, Liu N (2018) Modification of antibacterial ZnO nanorods with CeO_2 nanoparticles: role of CeO_2 in impacting morphology and antibacterial activity. Colloid Interface Sci Commun 26:32
3. Pomorska A, Grundmeier G, Ozcan O (2014) Effect of Zn^{2+} concentration on the adsorption of organophosphonic acids on nanocrystalline ZnO surfaces. Colloid Interface Sci Commun 2:11
4. Alswat A, Ahmad M, Saleh T (2017) Preparation and characterization of zeolite\zinc oxide-copper oxide nanocomposite: antibacterial activities. Colloid Interface Sci Commun 16:19
5. Kaushal S, Sharma P, Mittal S, Singh P (2015) A novel zinc oxide–zirconium(IV) phosphate nanocomposite as antibacterial material with enhanced ion exchange properties. Colloid Interface Sci Commun 7:1
6. Zhou J, Wu X, Xiao D, Zhuo M, Jin H (2017) Deposition of aluminum doped ZnO as electrode for transparent ZnO/glass surface acoustic wave devices. Surf Coat Technol 320:39
7. Hoffmann S, Albert M, Weber N, Sievers D, Meier C (2018) Tailored UV emission by nonlinear IR excitation from ZnO photonic crystal nanocavities. ACS Photonics 5(5):1933
8. Li H, Zhao W, Yi C, Xiong L, Gao Y (2019) High-level-Fe-doped P-type ZnO nanowire array/n-GaN film for ultraviolet-free white light-emitting diodes. Mater Lett 239:45
9. Tyona M, Jambure S, Lokhande C, Ezema F (2018) Dye-sensitized solar cells based on Al-doped ZnO photoelectrodes sensitized with rhodamine. Mater Lett 220:281
10. Mousavi S, Sajad B, Majlesara M (2019) Fast response ZnO/PVA nanocomposite-based photodiodes modified by graphene quantum dots. Mater Des 162:249
11. Vittal R, Hoa K-C (2017) Zinc oxide based dye-sensitized solar cells: a review. Renew Sustain Energy Rev 70:920
12. Ashkarran A (2012) A twice liquid arc discharge approach for synthesis of visible-light-active nanocrystalline Ag:ZnO photocatalyst. Appl Phys A 107:401
13. Wang L, Kang Y, Liu X, Zhang S, Huang W, Wang S (2012) ZnO nanorod gas sensor for ethanol detection. Sens Actuators, B 162(1):237
14. Suematsu K, Watanabe K, Tou A, Sun Y, Shimanoe K (2018) Ultraselective toluene-gas sensor: nanosized gold loaded on zinc oxide nanoparticles. Anal Chem 90(3):1959
15. Tian H, Fan H, Ma J (2018) Pt-decorated zinc oxide nanorod arrays with graphitic carbon nitride nanosheets for highly efficient dual-functional gas sensing. J Hazard Mater 341:102
16. Rambu A, Ursu L, Iftimie N, Nica V, Dobromir M, Lacomi F (2013) Study on Ni-doped ZnO films as gas sensors. Appl Surf Sci 280:598
17. Ramalingam R (2012) Polymer assisted Ga doped ZnO nanodisk/nanorod structures prepared by a low temperature one-pot hydrothermal method. Mater Lett 68:247

18. Shen Y, Bi H, Li T, Zhong X, Chen X, Fan A, Wei D (2018) Low-temperature and highly enhanced NO_2 sensing performance of Au-functionalized WO_3 microspheres with a hierarchical nanostructure. Appl Surf Sci 434:922
19. Zhao S, Shen Y, Yan X, Zhou P, Yin Y, Lu R, Han C, Cui B, Wei D (2019) Complex-surfactant-assisted hydrothermal synthesis of one-dimensional ZnO nanorods for high-performance ethanol gas sensor. Sens Actuators, B 286:501
20. Chen X, Shen Y, Zhou P, Zhao S, Zhong X, Li T, Han C, Wei D (2019) NO_2 sensing properties of one-pot-synthesized ZnO nanowires with Pd functionalization. Sens Actuators, B 280:151
21. Zhu Hongliang, Yang Deren, Zhang Hui (2006) A simple and novel low-temperature hydrothermal synthesis of ZnO nanorods. Inorg Mater 42(11):1210
22. Zhang Hui, Yang Deren, Ji Yujie, Ma Xiangyang, Jin Xu, Que Duanlin (2004) Low temperature synthesis of flowerlike ZnO nanostructures by cetyltrimethylammonium bromide-assisted hydrothermal process. J Phys Chem B 108(13):3955
23. Thilagavathi T, Geetha D (2013) Low-temperature hydrothermal synthesis and characterization of ZnO nanoparticles. Indian J Phys 87(8):747
24. Yang JH, Zheng JH, Zhai HJ, Yang LL (2009) Low temperature hydrothermal growth and optical properties of ZnO nanorods. Cryst Res Technol 44(1):87
25. Phromyothin D, Phatban P, Jessadaluk S, Khemasiri N, Kowong R, Vuttivong S, Pornthreeraphat S, Chananonnawathorn C, Horphathum M (2017) Growth of ZnO nanorods via low temperature hydrothermal method and their application for hydrogen production. Mater Today Proc 4:6326
26. Patil J, Nadargi D, Suryavanshi S (2014) Glycine combusted $ZnFe_2O_4$ gas sensor: Evaluation of structural, morphological and gas response properties. Ceram Int 40(7):10607
27. Kandula S, Jeevanandam P (2015) Sun-light-driven photocatalytic activity by ZnO/Ag heteronanostructures synthesized via a facile thermal decomposition approach. RSC Adv 5:76150
28. Li Y, Qiao L, Wang LL, Zeng Y, Fu WY, Yang HB (2013) Synthesis of self-assembled 3D hollow microspheres of SnO_2 with an enhanced gas sensing performance. Appl Surf Sci 285:130
29. Wang BB, Fu XX, Liu F, Shi SL, Cheng JP, Zhang XB (2014) Fabrication and gas sensing properties of hollow core–shell SnO_2/α-Fe_2O_3 heterogeneous structures. J Alloys Compd 587:82
30. Patil J, Nadargi D, Mulla I, Suryavanshi S (2018) Spinel $MgFe_2O_4$ thick films: a colloidal approach for developing gas sensors. Mater Lett 213:27
31. Mehta S, Nadargi D, Mulla I, Suryavanshi S (2018) Ru loaded mesoporous WO_3 microflowers for dual applications: enhanced H_2S sensing and sunlight driven photocatalysis. Dalton Trans 47:16840
32. Sharma SK, Ghodake GS, Kim D, Thakur O (2018) Synthesis and characterization of hybrid Ag–ZnO nanocomposite for the application of sensor selectivity. Curr Appl Phys 18:377
33. Wang Z, Liu L (2009) Synthesis and ethanol sensing properties of Fe-doped SnO_2 nanofibers. Mater Lett 63(11):917
34. Hjiri M, Mir L, Leonardi S, Pistone A, Mavilia L, Neri G (2014) Al-doped ZnO for highly sensitive CO gas sensors. Sens Actuators, B 196:413
35. Park S, An S, Mun Y, Lee C (2013) UV-enhanced NO_2 gas sensing properties of SnO_2-Core/ZnO-shell nanowires at room temperature. ACS Appl Mater Interfaces 5(10):4285
36. Xia J, Diao K, Zheng Z, Cui X (2017) Porous Au/ZnO nanoparticles synthesised through a metal organic framework (MOF) route for enhanced acetone gas-sensing. RSC Adv 7:38444
37. Jia Q, Ji H, Zhang Y, Chen Y, Sun X, Jin Z (2014) Rapid and selective detection of acetone using hierarchical ZnO gas sensor for hazardous odor markers application. J Hazard Mater 276:262
38. Al-Hardan NH, Abdullah MJ, Abdul-Aziz A (2013) Performance of Cr-doped ZnO for acetone sensing. Appl Surf Sci 270:480
39. Li XB, Ma SY, Li FM, Chen Y, Zhang QQ, Yang XH, Wang CY, Zhu J (2013) Porous spheres-like ZnO nanostructure as sensitive gas sensors for acetone detection. Mater Lett 100:119
40. Liu L, Li S, Zhuang J, Wang L, Zhang J, Li H, Liu Z, Han Y, Jiang X, Zhang P (2011) Improved selective acetone sensing properties of Co-doped ZnO nanofibers by electrospinning. Sens Actuators B155:782
41. Nath SS, Choudhury M, Chakdar D, Gope G, Nath RK (2010) Acetone sensing property of ZnO quantum dots embedded on PVP. Sens Actuators, B 148:353
42. Peng C, Guo J, Yang W, Shi C, Liu M, Zheng Y, Xu J, Chen P, Huang T, Yang Y (2016) Synthesis of three-dimensional flower-like hierarchical ZnO nanostructure and its enhanced acetone gas sensing properties. J Alloys Compd 654:371
43. Qi Q, Zhang T, Liu L, Zheng X, Yu Q, Zeng Y, Yang H (2008) Selective acetone sensor based on dumbbell-like ZnO with rapid response and recovery. Sens Actuators, B 134:166
44. Rahman M, Khan SB, Asiri AM, Alamry KA, Parwaz-Khan AA, Khan A, Rub MA, Azum N (2013) Acetone sensor based on solvothermally prepared ZnO doped with Co_3O_4 nanorods. Mikrochim Acta 180:675
45. Sahay P (2005) Zinc oxide thin film gas sensor for detection of acetone. J Mater Sci 40:4383
46. Chang S, Hsueh T, Chen I, Hsieh S, Chang S, Hsu C, Lin Y, Huang B (2008) Highly sensitive ZnO nanowire acetone vapor sensor with Au adsorption. IEEE Trans Nanotechnol 7:754
47. Song P, Wang Q, Yang Z (2012) Acetone sensing characteristics of ZnO hollow spheres prepared by one-pot hydrothermal reaction. Mater Lett 86:168
48. Wang X, Wang W, Liu Y (2012) Enhanced acetone sensing performance of Au nanoparticles functionalized flower-like ZnO. Sens Actuators, B 168:39
49. Wei S, Zhou M, Du W (2011) Improved acetone sensing properties of ZnO hollow nanofibers by single capillary electrospinning. Sens Actuators, B 160:753
50. Xu X, Chen Y, Ma S, Li W, Mao Y (2015) Excellent acetone sensor of La-doped ZnO nanofibers with unique bead-like structures. Sens Actuators, B 213:222
51. Zeng Y, Zhang T, Yuan M, Kang M, Lu G, Wang R, Fan H, He Y, Yang H (2009) Growth and selective acetone detection based on ZnO nanorod arrays. Sens Actuators B143:93